Taylor & Francis
Taylor & Francis Group

Automatika

Journal for Control, Measurement, Electronics, Computing and Communications

ISSN: (Print) (Online) Journal homepage: www.tandfonline.com/journals/taut20

Experimental study and techno-economic evaluation of an active fault detection kit in the prospect of future zero energy building installations

Christos Pechlivanis, Nick Rigogiannis, Andreas Tichalas, Faidra Kotarela & Nick Papanikolaou

To cite this article: Christos Pechlivanis, Nick Rigogiannis, Andreas Tichalas, Faidra Kotarela & Nick Papanikolaou (2024) Experimental study and techno-economic evaluation of an active fault detection kit in the prospect of future zero energy building installations, Automatika, 65:4, 1469-1486, DOI: 10.1080/00051144.2024.2390328

To link to this article: https://doi.org/10.1080/00051144.2024.2390328

© 2024 The Author(s). Published by Informa UK Limited, trading as Taylor & Francis Group.

Published online: 29 Aug 2024.

Submit your article to this journal

Article views: 281

View related articles

View Crossmark data

Full Terms & Conditions of access and use can be found at
https://www.tandfonline.com/action/journalInformation?journalCode=taut20

AUTOMATIKA
2024, VOL. 65, NO. 4, 1469–1486
https://doi.org/10.1080/00051144.2024.2390328

OPEN ACCESS Check for updates

Experimental study and techno-economic evaluation of an active fault detection kit in the prospect of future zero energy building installations

Christos Pechlivanis, Nick Rigogiannis, Andreas Tichalas, Faidra Kotarela and Nick Papanikolaou

Department of Electrical and Computer Engineering, Democritus University of Thrace, Xanthi, Greece

ABSTRACT

This article presents an active fault detection kit, applicable to low voltage single-phase electrical installations, in the prospect of the Zero Energy Building concept, integrating on-site renewable energy generation and energy storage. This simple, flexible, self-powered and compact kit is capable of detecting faults, such as power theft (meter tampering), unintentional islanding and neutral conductor loss. Its operation is based on harmonic voltage injection, in series with the electrical installation, through a low-power H-bridge inverter and a current transformer, along with the corresponding harmonic current measurement, to estimate the impedance and effectively detect faulty conditions; the fast and robust Goertzel algorithm is utilized. Moreover, it features IoT communication capabilities, employing the ESP32 microcontroller, to exchange data and information with the installation meters. The functionality and effective fault detection of the proposed device are validated, through experimental tests on a custom-developed hardware prototype; IoT connectivity and data uploading are experimentally tested and verified, too. Finally, a sustainability assessment study is performed, using the Life Cycle Cost Analysis tool.

ARTICLE HISTORY
Received 16 February 2024
Accepted 23 July 2024

KEYWORDS
Active fault detection; building electrical installations; harmonic injection; impedance estimation; Internet of Things; Life Cycle Cost Analysis

1. Introduction

Ensuring a reliable and secure electricity distribution system is crucial nowadays, given the widespread adoption of renewables and energy storage in low-voltage electrical installations. This urge is influenced by directives from the European Union (EU) and stringent short-term targets for modern building installations (e.g. residential, commercial, industrial) to substantially reduce power demands and CO_2 emissions, thereby enhancing energy efficiency and advancing the concept of the Zero Energy Building (ZEB) [1–3]. However, notable challenges are still evident, including issues like meter tampering (found also as power or electricity theft), unintentional islanding, and the loss of neutral conductor, all of which pose threats to the safety of both the power system and human life [4–16].

In this light, the development of a holistic active fault detection solution (kit) for modern and future building installations seems imperative, due to the intense presence of the so-called load-matching conditions in an electrical installation, that will rise in the context of ZEBs (i.e. prosumer buildings incorporating local generation and energy storage); indeed, due to the fact that future ZEBs will have to serve considerably higher amounts of electric loads (for heating and cooling purposes, electric vehicle charging, etc.) and the fact that the relevant EU directives [17] impose the mass installation of battery units in buildings (to reduce energy transactions with the utility grid), it is concluded that future ZEBs will have more balanced loads (i.e. in terms of local generation and demand).

The proposed kit has been initially presented in [15], to effectively detect the previously mentioned faulty conditions. The first one is the neutral conductor loss, which may result in serious consequences for the consumers and the electrical installations. According to [4–6,15,16], such an event may provoke the development of dangerous voltage potential on exposed conductive parts as well as being harmful for the connected loads, due to overvoltages. In addition, islanding condition takes place when the ZEB installation (renewable distributed generation, energy storage units and loads) operates isolated from the distribution network, raising additional hazards to both the safety of individuals and of the electrical infrastructure. As a result, the incorporation of an anti-islanding technique has become obligatory, according to IEEE Std.1547.1, IEEE Std. 929-2000, and UL1741 standards [10–13,15,16,18]. Finally, meter tampering is regarded as an increase in unforeseen load demand, potentially leading to equipment overloading within the power grid, voltage fluctuations, and escalated electricity production expenses. From an economic perspective, global power theft is responsible for losses of roughly 89 billion USD annually, as indicated by a study conducted by Northeast Group LLC [19]. The rapid growth of this issue is attributed, on one hand, to prolonged economic downturns, which has encouraged illegal behaviours, whereas on the other

CONTACT Nick Papanikolaou npapanik@ee.duth.gr

© 2024 The Author(s). Published by Informa UK Limited, trading as Taylor & Francis Group.
This is an Open Access article distributed under the terms of the Creative Commons Attribution License (http://creativecommons.org/licenses/by/4.0/), which permits unrestricted use, distribution, and reproduction in any medium, provided the original work is properly cited. The terms on which this article has been published allow the posting of the Accepted Manuscript in a repository by the author(s) or with their consent.

hand, to the delayed implementation of a legal framework to address the problem effectively. Consequently, in developing nations, where energy costs are relatively high and electricity bills may be unmanageable, many individuals seek to avoid payment for the electricity they consume. Similarly, due to the lack of a robust legal framework to tackle the issue, some individuals may continue to engage in this unlawful activity.

Similar solutions have been proposed in recent scientific literature, to address the issues of power theft and neutral conductor loss, whereas the islanding detection matter is primarily assigned and integrated to the control scheme of the distributed generator (DG) inverter [4–12,14–16]. Such systems use various methods to identify and prevent unauthorized consumption of electricity, mainly through the recording and processing of meter data. Those advanced metering systems comprise smart meters, communication networks and data management algorithms. They collect and analyse data from meters, to detect inconsistencies and anomalies that may indicate electricity theft, providing detailed reports and alerts to the user and the utility companies. Various systems have been proposed utilizing different techniques, i.e. tamper detection sensors, installed on meters or distribution equipment to detect physical tampering attempts and send alerts [20–27], power line communication, to monitor electricity flow and detect unauthorized usage or tampering along the power lines [28], or advanced solutions based on machine learning and AI algorithms (e.g. neural networks), to analyse large datasets from meters and other sources to identify patterns indicative of power theft and predict potential theft locations, based on historical data and other factors [29–38]. It is noted that several of the proposed solutions incorporate Internet of Things (IoT) technology, to facilitate connectivity and communication with other smart devices [39,40].

As regards the commercially available solutions, even though the market of such devices was limited until recently, several companies (e.g. Siemens, Honeywell, Schneider Electric, Texas Instruments) offer solutions that provide smart grid and installation management, including a form of power theft detection [41–48]. For instance, Schneider Electric provides various Energy Meter Kits, which constitute compact energy management solutions, whereas their specially designed enclosure protects the smart meters from tampering attempts [44]. A similar solution has been developed by Texas Instruments, featuring a special smart meter design, incorporating inductive sensors to accurately and reliably determine if the meter case has been opened, alerting service providers for a possible power theft attack [47,48]. Regarding the data-driven approach, the EnergyIP® Meter Data Management Revenue Protection system, provided by Siemens, utilizes algorithms to analyze meter data and identify non-technical losses and issues with power quality, whereas it is also capable to take decisions and act on critical data [41]. Finally, several examples of this category have been developed by startups. One of the most successful is the case of Bidgely, that developed the UtilityAI® Energy Theft Detection system, which is an AI-based accurate power theft detection solution. It utilizes non-intrusive load monitoring and advanced data analytics, and it can drill down to the premises level, discovering theft patterns in behind-the-meter energy consumption to find tariff misuse, direct theft, meter tampering, and other non-technical loss [45].

However, except for the aforementioned advanced capabilities, existing solutions also come with certain limitations and drawbacks. At first, a significant disadvantage is the high initial costs, since the deployment of advanced metering infrastructure involves significant upfront investment in hardware, software, and installation. In parallel, existing infrastructure may need upgrades to support new technologies, adding to the costs. Apparently, in case of deploying such systems in rural or remote areas with limited infrastructure and connectivity can be really challenging and in some cases cost-prohibitive. Finally, regular maintenance (along with technical support) and updates are required, to ensure the proper functioning of these systems, adding to operational costs.

Moreover, personal data privacy and security concerns are raised, as smart meters collect detailed consumption data, whilst the interconnected nature of smart grids makes them vulnerable to cyberattacks, which can lead to data breaches or disruptions in power supply. In addition, the complexity in implementation is increased, since the incorporation of new technologies with legacy systems can be challenging and may require substantial modifications. Another major drawback is related to data volume and management, since the above-described data-driven systems generate vast amounts of data, which require robust data management systems to process, store, and analyze effectively. In parallel, it is noted that data analysis requires high computational resources and sophisticated algorithms. Last but not least, it is noted that those detection systems may sometimes generate false positives (false alarms) or false negatives (missed detections), leading to reliability issues and operational inefficiencies.

To sum up, as it is discussed above, smart meters and similar fault detection devices have been proven to be effective in counteracting various forms of power theft to a certain extent; although they lack the capability to reliably identify theft attempts involving simultaneous bridging of the input-output of one or more phases and neutral terminals, whereas they do not provide overall fault detection for the electrical installation, in a simple, direct manner [4–16,20–40]. Therefore, the creation of an integrated intelligent system capable of detecting undesirable operating conditions such as power theft, islanding and neutral loss is paramount, to guarantee

the reliable and secure functioning of the distribution network, as well as to safeguard human life.

In this context, this paper aims to experimentally investigate the performance of a flexible active fault detection kit, along with its wireless communication capabilities, as well as to evaluate its sustainability through the well-established Life Cycle Cost Analysis (LCCA) method. To extend the solution presented in [15], improve its performance and include advanced communication capabilities, the contribution of this work can be summarized as follows:

- For the impedance estimation process, the fast and robust Goertzel algorithm is selected, which is proved to be advantageous, compared to the commonly used Fast Fourier Transform (FFT).
- The wireless communication capabilities (through Wi-Fi protocol) of the selected ESP32 microcontroller are fully exploited and experimentally tested, in the context of the emerging Internet of Things (IoT) connectivity, for smart household installations.
- The sustainability of the studied active fault detection kit (i.e. analysis of the system present value and definition of the overall cost over its lifetime, based on realistic maintenance costs, energy price rates, as well as financial parameters, such as the inflation, the discount rate etc.) is estimated, through LCCA calculations.

In general, the studied device provides a robust solution for active (via harmonic injection) detection of neutral loss, islanding and meter tampering, by monitoring the line impedance of the electrical installation in order to evaluate its condition. Each impedance value corresponds to a specific system state (i.e. normal, islanding, neutral loss and power theft), according to predefined impedance limits. The kit is designed to be both compact and flexible during installation, while it includes its own battery, ensuring uninterrupted operation. Moreover, it features wireless connectivity, enabling information/data exchange and coordination with several devices such as smart meters, sensors, and microcontrollers within the ZEB installation. Consequently, this device is characterized by its intelligence and flexibility, facilitating the integration of DG units, such as building-integrated and/or applied photovoltaic modules, into the electricity grid (through the ZEB concept), thereby fostering a more sustainable distribution network. Regarding the selected Goertzel algorithm for the monitoring of the line impedance, it is capable of determining both magnitude and phase of a specific harmonic frequency by analysing the measured voltage and current signals. Although the Goertzel is more complex than the FFT algorithm, it is proven to be more numerically efficient for calculating a small number of selected frequency components, resulting in faster execution. Additionally, its simple structure makes it suitable for use in small processors and microcontroller applications [49]. In this study, the magnitudes of 600 Hz (12th harmonic – injected) and 50 Hz (fundamental) current and voltage signals are extracted. This enables the detection of faulty conditions based on the 600 Hz impedance value and the estimation of installation consumption by using the 50 Hz current/voltage values.

Finally, it is important to highlight that the fault detection kit is applicable to all LV electrical installation types, including residential, industrial, and commercial setups, regardless of whether they are single-phase or 3-phase and irrespective of nominal fundamental voltage and frequency values. It is also compatible with TN/TT networks. The single-phase prototype version is developed and experimentally studied in this work.

2. Theoretical background and system description

2.1. Features and fundamental principles of operation

The described detection kit is primarily intended for use in low voltage (LV) residential installations, which may or may not incorporate DG units. However, its utility can be generalized for building installations, i.e. industrial and commercial applications. Detection of meter tampering, islanding, and neutral loss is achieved through the injection of zero-sequence harmonic voltage components, applicable to both single-phase and multi-phase (M-phase, where $M \geq 1$) systems [11,12,15,16,50]. The fault detection kit comprises M-voltage sources, generated by a low-power inverter, interconnected in series with each phase of the electrical installation, resulting in a 12th order harmonic (or 600 Hz) voltage injection. The selection of the 12th harmonic order is made for practical reasons, as it is an uncommon harmonic order in power grids, minimizing so any potential interference in measurements. Additionally, the relevant power quality standard EN 50160, that governs power quality at the point of common coupling (PCC) on the supplier side, does not anticipate significant harmonic distortion for the 12th harmonic component [51], [52]. Specifically, this standard allows only a small percentage of even harmonic distortion (i.e. 0.5% for orders 6 through 24). Leveraging this favourable harmonic level enables the effective impedance estimation / monitoring without inducing notable voltage distortion; hence, no disturbances in the electricity network are expected. In case that communication protocols within the electrical installation coincide with the harmonic injection, an alternative harmonic order (such as 14th or 16th) with similar characteristics — unusual harmonic orders for electrical grids — can be employed, while adhering

to EN 50160 limits. The likelihood of causing additional issues in neighbouring installations using this protective approach is low, thanks to the use of series-connected (with the installation) high impedance voltage sources for harmonic injection, ensuring so adequate isolation among neighbouring injections. Consequently, this design yields a compact, robust, and safe device, ensuring the reliable impedance monitoring for accurate detection of the aforementioned unintentional events.

Additionally, it is important to highlight that the placement of the proposed kit and the type of grounding system are essential factors that must be considered [4]. Specifically, if the kit is installed in the same box with the power meter, it not only facilitates the detection of islanding and neutral conductor loss but it also enables the identification of electricity theft, commonly executed by bridging one or more phases of the energy meter. This is accomplished through continuous monitoring and estimation of the line impedance. Under such circumstances, the measured impedance tends to approach zero; similar behaviour is observed (the measured impedance becomes constant) when there a bypassing bridge (e.g. through inductors) exists across the device terminals.

On the other hand, if the kit is positioned elsewhere along the power line or the neutral conductor, its capacity to identify meter tampering may be compromised, while its capability to detect neutral loss and islanding remains unaffected. Consequently, if phase bridging occurs at the power meter, the device may fail to detect meter tampering. To optimize its overall performance across all operating scenarios and uphold its power theft detection functionality, it is suggested to install the device near the energy meter. This placement also leverages its Wi-Fi connectivity features for data exchange with the meter. Any disparities in measured quantities or detected events can be transmitted via signal to a remote central controller (server) for local storage and further analysis. Thus, careful consideration of the detection kit placement is essential, to ensure reliable Wi-Fi communication with the smart power meter.

A block diagram of the proposed kit integration, along with the equivalent schematic diagram of its power stage, comprising a DC voltage source (battery power cell) an H-bridge inverter, an output low pass filter (LPF), a current transformer and a parallel branch (capacitor in series with a TRIAC switch), are depicted in Figure 1. It is noted that the battery is charged through the grid (electrical installation connection), by means of the current transformer and the effective H-bridge bidirectional operation, leading to a self-powered device. In addition, the current transformer is in charge of the harmonic injection into the installation line. The low impedance winding of the transformer is connected in series with the installation phase, whereas the harmonic voltage source is connected to the high impedance winding. This link guarantees that the power flow at the fundamental frequency remains unaffected when injecting harmonic voltage components. Moreover, voltage and current sensors are installed to precisely measure the injected voltage ($V_{inj,h}$) and current ($i_{inj,h}$) components, essential for impedance calculation.

The fundamental equations describing the harmonic voltage source for continuous or discontinuous injection in each phase, within a generalized M-phase system, are deduced as follows:

$$V_{inj,h}(i,t) = \sqrt{2}A_{inj}(i)\sin(h\omega_g t) \tag{1}$$

$$V_{inj,h}(\mathrm{i,k,t}) = \sum_{k=1}^{Q}[u(t-t_{i,k}) - u(t-\Delta t_{i,k} - t_{i,k})]\cdot \sqrt{2}A_{inj}(\mathrm{i,k})\sin(h(\mathrm{k})\omega_g \mathrm{t}) \tag{2}$$

where $i = 1, 2, \ldots M$, $k = 1, 2, \ldots Q$, ω_g is the grid frequency, M is the number of system phases, h is the order of the harmonic injection, Q is the number of injected harmonic components, $A_{inj(i,k)}$ is the amplitude of the injected voltage components, $t_{i,k}$ is the starting time point of the $h(k)$ harmonic injection at the i-branch and $\Delta_{ti,k}$ is the time period of the $h(k)$ injection at the i^{th} branch.

Moreover, Figure 2 illustrates the equivalent sche matic diagram of the zero-sequence circuit for a single-phase setup. While this setup can be extended to M-phase configurations without notable distinctions, it is important to highlight that in single-phase systems the zero-sequence voltage is naturally zero. Consequently, this absence of zero-sequence voltage leads to $V_{Line,0seq,h} = 0$. To expand on this, the zero-sequence load and grid impedance will remain unaffected and will adhere to:

- $Z_{g,h}$: the magnitude of the h-harmonic impedance of the grid,
- $Z_{L,h}$: the magnitude of the h-harmonic load impe dance.

Considering the potential occurrence of a zero-load situation, where the proposed device may encounter a resistance ranging from very high values to nearly infinite, it is vital to integrate a mechanism capable of distinguishing such cases from islanding conditions. Therefore, to detect zero-load conditions, a parallel branch is introduced, comprising a TRIAC switch (S_p) and a relatively high impedance value ($Z_{p,h}$) at the fundamental 50 Hz frequency. The operating principle of this mechanism is straightforward; upon detecting a notably high grid impedance (which may be due to open circuit, low load or islanding conditions), the device commands the closing of the switch, isolating the load. Subsequently, the line impedance is recalculated at

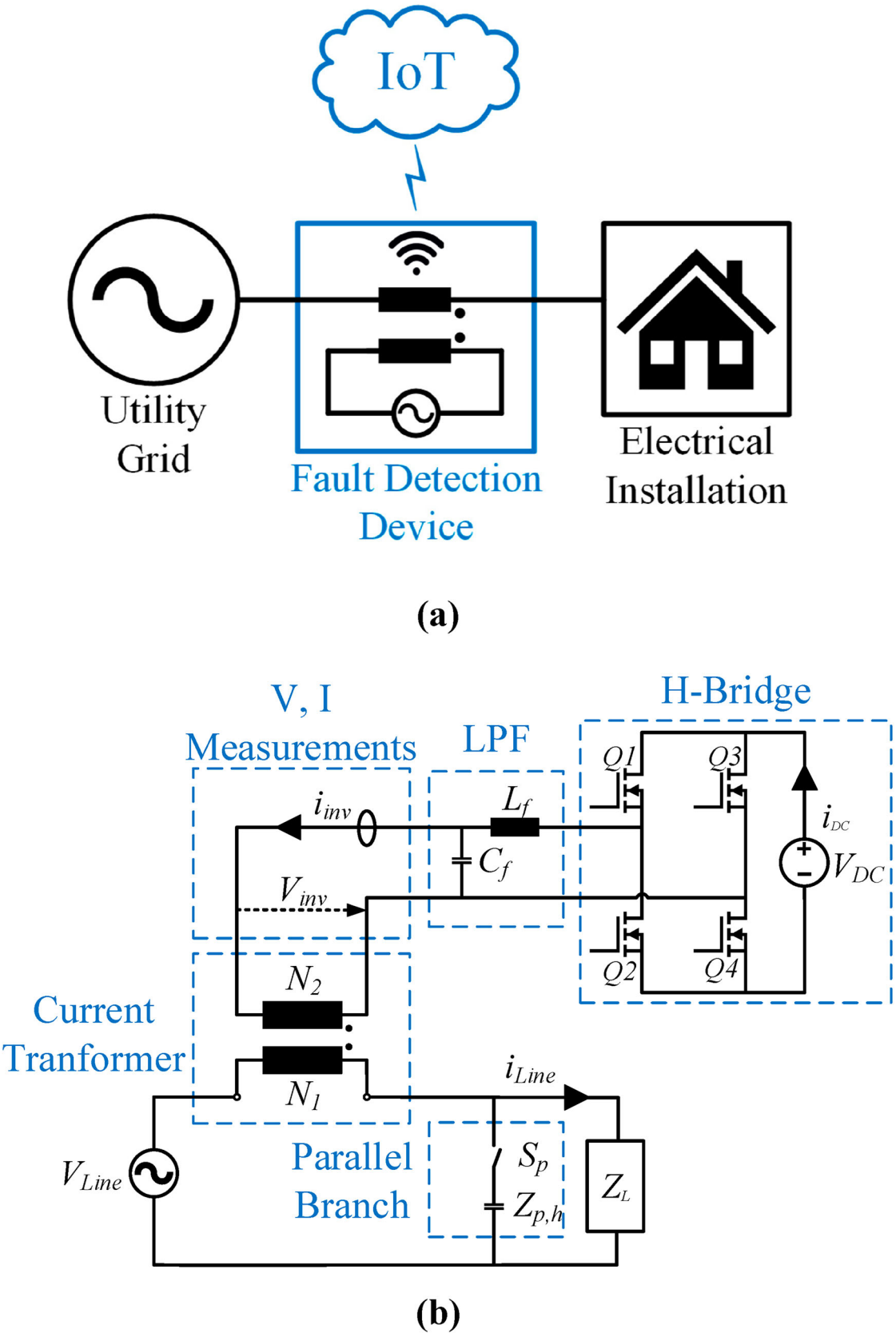

Figure 1. The incorporation of the single-phase active fault detection device into an electrical installation; (a) block diagram, (b) schematic diagram of its power stage.

predetermined intervals. This iterative process enables the verification of whether the impedance falls within acceptable limits, defined by adding the line impedance $Z_{g,h}$ to the impedance of the parallel branch $Z_{p,h}$. If the total impedance remains within the acceptable range, it indicates the presence of a zero-load scenario.

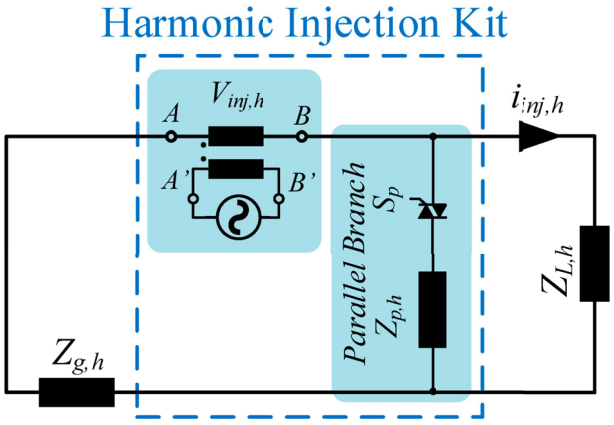

Figure 2. Equivalent harmonic zero sequence model of a single-phase system.

2.2. Fault detection, evaluation and controller design

The detection of both neutral loss and islanding for a generalized M-phase installation can be achieved through the utilization of mathematical tools, such as the FFT [12], or the advanced Goertzel algorithm, selected in this work. According to these methods, the voltage and current signals from the injection circuit are fed to a transformation block, to derive the corresponding RMS values of the harmonic components [11–13,50]. In the context of single-phase installations, the corresponding zero-sequence values align with the RMS values, obtained from the measured voltage ($V_{inj,h}$) and current ($i_{inj,h}$), by the proposed kit. This results to simpler estimation of the grid impedance and thus to faster detection of unintentional events. As a result, the total line impedance shall be:

$$Z_{tot,h} = \frac{V_{inj,h}}{I_{inj,h}} \tag{3}$$

where $Z_{tot,h}$ is the total calculated line impedance (e.g. $Z_{g,h} + Z_{L,h}$ in case that S_p is open and $Z_{g,h} + Z_{p,h}$ in case that S_p is closed).

To effectively distinguish between normal grid operation and abnormal scenarios, such as neutral conductor loss and islanding, the grid impedance is compared to specific predetermined threshold values, namely NO_{Ulim} and ND_{Ulim}, as illustrated in Figure 3. The determination of NO_{Ulim} corresponds to realistic grounding resistance values, in cases of loss of neutral for the experimental setup and involves some experimental testing, in which the noise and the accuracy of the measuring instruments should be taken into account. Additionally, the ND_{Ulim} corresponds to practical impedance values of islanded loads.

Apparently, a calibration process during the initial installation of the studied kit is necessary, to ensure its reliable and precise operation. In any case, those limits can be adapted to the specific features of the installations under consideration. However, it is worth

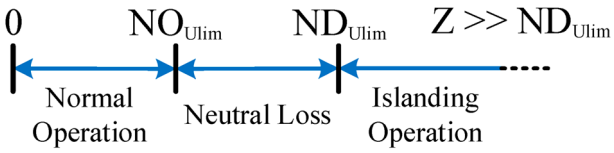

Figure 3. Fault detection threshold values for each faulty condition.

noting that these values remain within a specific range for building installations within a specific geographical region (i.e. thanks to similar soil characteristics, such as resistivity, moisture, temperature etc.). Last but not least, it is noted that the proposed digital control implementation using the ESP32 microcontroller provides a simple firmware update process, by means of the Wi-Fi communication, without the need for a USB connection to a computer. This feature facilitates any necessary modifications to the aforementioned threshold values, in case of potential changes in the electrical installation characteristics or user demands.

Impedance data falling between the NO_{Ulim} and N_{DUlim} thresholds indicate a neutral loss event, while data surpassing the ND_{Ulim} threshold indicate an islanding situation. This methodology allows for the detection of both islanding and neutral loss, even under load matching conditions in ZEB installations, where DG units are connected in parallel with the local load $Z_{L,h}$.

On the other hand, electricity theft is achieved by bridging one or more phases of the energy meter, causing a short-circuit of the harmonic voltage source $V_{inj,h}$, leading to the generation of short-circuit currents and voltage drop. As a result, the measured impedance tends towards zero, since the current reaches very high levels. In such instances, the fault detection kit alerts the user about the detection of power theft. Consequently, the device voltage and current are as follows:

$$I_{inj,SC} \gg I_{inj,h} \tag{4}$$

$$V_{inj,SC} \to 0 \tag{5}$$

where $I_{inj,SC}$ and $V_{inj,SC}$ are the magnitudes of the h^{th} harmonic short circuit current and voltage, when meter tampering occurs.

As regards the impedance estimation technique, compared to the typically utilized FFT [15,16,50], the Goertzel algorithm is employed in this work. It constitutes a robust digital signal processing technique, used to extract the magnitude and phase of the desired frequency from an input signal, with minimum computational burden [49]. Furthermore, this algorithm has been widely proposed for active islanding detection techniques [11,49,53]. Specifically, the algorithm is used to compute the Digital Fourier Transform (DFT) spectra. It can be applied either from the perspective of the DFT over short time sections of the signal (with fixed time window), or from the perspective of

Table 1. Comparison of the required mathematical operations count for common impedance estimation algorithms.

Algorithm	Multiplications	Additions
FFT	$Nlog_2N$	–
DFT	$2N$	$2N$
Goertzel	$N+2$	$2N+1$

a filtering process at a specific (fixed) frequency. In parallel, it is a faster method of pitch detection than the FFT and the DFT for a single frequency [53]. In particular, Table 1 presents a comparison of the required mathematical operations count for FFT, DFT and Goertzel [12,49]. The detailed mathematical analysis, along with the timing process and the block diagram of the Goertzel algorithm can be found in [12]. In this work, only the z-domain fundamental equations are presented, as they are used for the digital implementation in the microcontroller unit; the ESP32 microcontroller is used, which integrates both Wi-Fi and Bluetooth connectivity.

In this paper, by employing the Goertzel algorithm, the magnitude of the fundamental (50 Hz) and the higher order (600 Hz) harmonic components are obtained, through the voltage and current measurements at the current transformer secondary side (H-bridge inverter side). The Goertzel algorithm z-domain transfer function is:

$$H(z) = \frac{1 - e^{-j\frac{2\pi k}{N}} z^{-1}}{1 - \cos\left(\frac{2\pi k}{N}\right) z^{-1} + z^{-2}} \tag{6}$$

The algorithm is applied in the form of a second-order discrete-time causal linear infinite-impulse-response filter. Therefore, the input-output behaviour of the filter can be treated as a set of linear difference equations, as:

$$x[n] = u[n] - 2\cos\left(\frac{2\pi k}{N}\right) u[n-1] + u[n-2] \tag{7}$$

$$u[n] = x[n] + 2\cos\left(\frac{2\pi k}{N}\right) u[n-1] - u[n-2] \tag{8}$$

$$y[n] = u[n] - u[n-1]e^{-j\frac{2\pi k}{N}} \tag{9}$$

where: *u[n]* is the intermediate value of the current *(n)* sampling time, *u[n-1]* is the intermediate value of the previous *(n-1)* sampling time, *u[n-2]* is the intermediate value of the *(n-2)* sampling time and *y[n]* is the complex value of the calculated signal.

The magnitude and phase of the calculated signal are derived by the following expressions:

$$|Y[N]| = \sqrt{\begin{array}{c} u^2[N-1] + u^2[N-2] \\ -2u[N-1]u[N-2]\cos\left(\frac{2\pi k}{N}\right) \end{array}} \tag{10}$$

$$\theta = \arctan\left(\frac{\sin\left(\frac{2\pi k}{N}\right) u[N-2]}{u[N-1] - \cos\left(\frac{2\pi k}{N}\right) u[N-2]}\right) \tag{11}$$

Following the application of the Goertzel algorithm on both voltage and current signals, the impedance of the 600 Hz line is determined and the outcome is uploaded to ThingSpeak, an Internet of Things analytics platform, facilitating real-time data collection, visualization, and analysis in the cloud. Additionally, utilizing the voltage and current data at 50 Hz, the power consumption of the electrical installation can be derived. These data are compared with the power calculations from the installation meter, via data exchange, to identify any notable disparities, thereby reducing the likelihood of power theft.

It is noted that the power consumption comparison does not have to be performed in real-time (e.g. it could be executed once every 15 min, whereas it is limited only by the smart meter and the fault detection kit computational features). Moreover, as long as both the compared values are characterized by a time stamp, transport delay does not matter, as the compared values have been recorded at the same time. Minor deviations (e.g. 1–2 sec) do not affect the comparison result, because no steep transients (e.g. in the millisecond scale) are expected in power consumption in real building installations. What is more, the comparison process can be executed by the microcontroller or the smart meter, whenever needed, since power consumption data are available online through IoT.

The designed controller flowchart, illustrating the overall operation of the fault detection device utilizing IoT is depicted in Figure 4. The system state estimation relies on two main factors: (a) the calculation of the 600 Hz impedance and (b) the comparison of power consumption with measurements from the installation meter, facilitated through communication. The smart detection device is able to alert the user regarding normal or abnormal operations by precisely identifying any faulty conditions.

Finally, it is noted that since this work focuses on the experimental validation and techno-economic assessment of the fault detection kit that has been proposed in [15], along with its upgrades (i.e. advanced impedance estimation via the Goertzel algorithm and wireless, IoT, communications capabilities), the modelling and simulation of the studied device are omitted. Nevertheless, the complete simulation study and verification of the proposed kit functionality (for all three fault cases, i.e. islanding, power theft and neutral loss) has been performed in [15], in MATLAB/Simulink, whereas the detailed mathematical analysis of the zero-sequence harmonic voltage injection for multi-phase systems has been presented in [16].

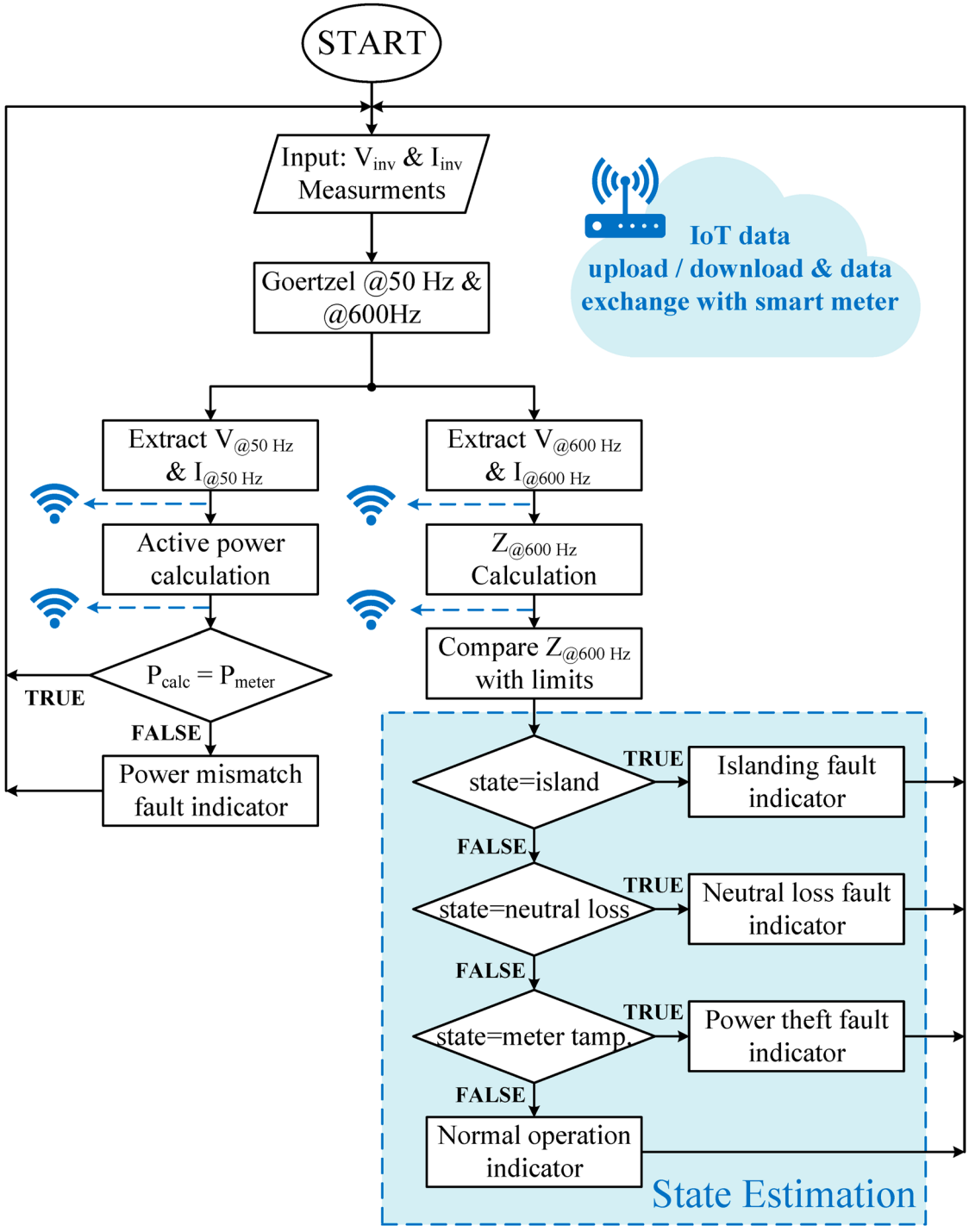

Figure 4. Flowchart of the designed control strategy for the active fault detection kit.

3. Hardware development and experimental results

3.1. Prototype development

To experimentally study and validate the effectiveness of the active fault detection kit, a prototype H-bridge inverter has been created. This inverter facilitates the introduction of the 12th harmonic voltage injection, applicable to single-phase electrical installations. The circuit board has been meticulously designed by the aid of the Altium Designer software suite, which is a professional-grade tool for Printed Circuit Board (PCB) development. Figure 5 presents a comprehensive 3D model of the board, offering intricate insights into its physical arrangement. In addition, Table 2 presents the complete Bill of Materials (BOM) for the designed kit, along with the respective cost for each component. It is noted that for the per-unit cost, the purchase of at least 1,000 items (quantity) of each component has been considered.

The compact nature of the developed device, its dimensions are 120 mm x 65 mm, primarily results from the utilization of miniature sized SMD components. It is crucial to emphasize the significance of its

Table 2. Complete Bill of Materials (BOM) for the developed fault detection kit, along with the respective cost for each component.

Manufacturer Part Number (MPN)	Description	Qty	Cost / Unit (€)	Total Cost (€)
TES 1-1212	isolated DC-DC converter 12 V/12V	1	4.9	4.9
TES 1-1211	isolated DC-DC converter 12 V/5V	1	5.2	5.2
LM7805SX/NOPB	linear voltage regulator	1	0.9	0.9
ESP32-DEVKITC-32D	microcontroller unit	1	9.4	9.4
LM358DR2G	operational amplifier	1	0.1	0.1
ACS730KLCTR-20AB-T	Hall-effect current sensor	1	2.5	2.5
NCP81075DR2G	bootstrap dual MOSFET gate driver	2	1.1	2.2
FDS6680AS	N-channel MOSFET	4	0.3	1.2
MOC3063	zero-cross optocoupler (phototriac)	1	0.2	0.2
B82801C0565A100	current transformer 1:100	1	1.8	1.8
691210910002	double headers	3	0.7	2.1
RL622-102K-RC	1 mH inductor	1	0.5	0.5
ASC1206-6R8FT5	6.8 Ω SMD resistor	4	0.1	0.4
CRCW25121K00FKEG	1 kΩ, 1 W, SMD resistor	5	0.1	0.5
MCPWR12FTEA1001	1 kΩ, 1.5 W, SMD resistor	4	0.1	0.4
CRCW251210K0FKEG	10 kΩ, 1 W, SMD resistor	2	0.1	0.2
C0805C103J3GACTU	10 nF, 25 V, ceramic SMD capacitor	1	0.1	0.1
12063C104MAT2A	0.1 μF, 25 V ceramic SMD capacitor	1	0.1	0.1
C0805C104K5RAC7411	0.1 μF, 50 V ceramic SMD capacitor	2	0.1	0.2
C4532X7R1H685K250KB	6.8 μF, 50 V, ceramic SMD capacitor	5	0.3	1.5
TPSD686K020R0150	68 μF, 20 V, tantalum SMD capacitor	7	0.9	6.3
Total				**40.7**

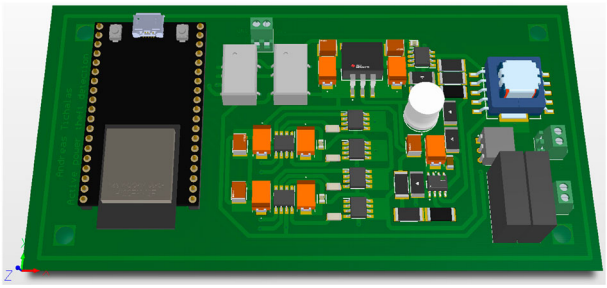

Figure 5. 3D illustration (top view) of the active fault detection kit PCB, obtained by Altium Designer platform.

size, particularly regarding the practical integration of such a kit into the electrical installations. Therefore, the reduced dimensions of the developed kit facilitate its versatile placement and incorporation into existing electrical panels with limited space. The developed kit is depicted in Figure 6, highlighting its primary elements. Engineered to operate with a single 12 V input source, such as a battery, it employs two built-in isolated DC-DC converters, i.e. TES 1-1212 and TES 1-1211, to provide 12 and 5 V outputs, respectively. These converters cater to the auxiliary power requirements of the main IC components, including the ESP32 microcontroller.

Regarding the driving circuitry for the H-bridge in this application, the most suitable solution seems to be the bootstrap supply driver. This choice is optimal considering factors such as size, cost, and complexity [54]. The commonly applied bootstrap technique involves the generation of a supply equivalent to the main power supply of the driving circuit (12 V in this case). This supply is responsible for providing the necessary turn-on charge to the MOSFET gates. Two NCP81075DR2G high-performance, non-isolated, dual gate drivers are employed. Additionally, the bootstrap diode is integrated into the driver IC, reducing the need for extra components and thus decreasing the overall size and cost of the device.

As for the parallel branch, a phototriac is selected instead of a typical TRIAC device. This decision is mainly driven by the low current requirements and compact size. An isolated MOC3063 zero-cross phototriac is selected as the most appropriate choice. The accurate calculation of the parallel branch impedance is crucial, as the current flowing through it must be kept significantly low (e.g. less than 1 A) for safe operation. By choosing a total capacitance of 94 nF (utilizing two 47 nF series-connected capacitors) and considering the reactance $X_c = 1/\omega C = 1/2\pi fC$, for a 50 Hz electricity grid, the expected parallel branch current is limited to 3 mA, well under 1 A.

For current measurement circuitry, the precise, low-offset, linear Hall sensor ACS730KLCTR-20AB is chosen, capable of generating an analogue voltage signal and conducting current measurements up to 20 A. Voltage measurement is achieved through a simple voltage divider, followed by a signal conditioning circuit to adjust signal amplitude and offset, based on the LM358DR2G operational amplifier.

Finally, to ensure the H-bridge generates a pure sinusoidal voltage waveform, a LPF is designed with a cutoff frequency set at 2 kHz (i.e. 10 times lower than the inverter switching frequency) by appropriately selecting L and C values, which are 1 mH and 6.8 μF, respectively. The bipolar SPWM technique is digitally implemented, by the aid of the ESP32 microcontroller, resulting in a 600 Hz sinusoidal waveform in the H-bridge output, after the LPF.

3.2. *Experimental validation – Indicative results*

An experimental setup at laboratory scale has been developed, to assess the functionality and communication capabilities of the studied system, featuring the

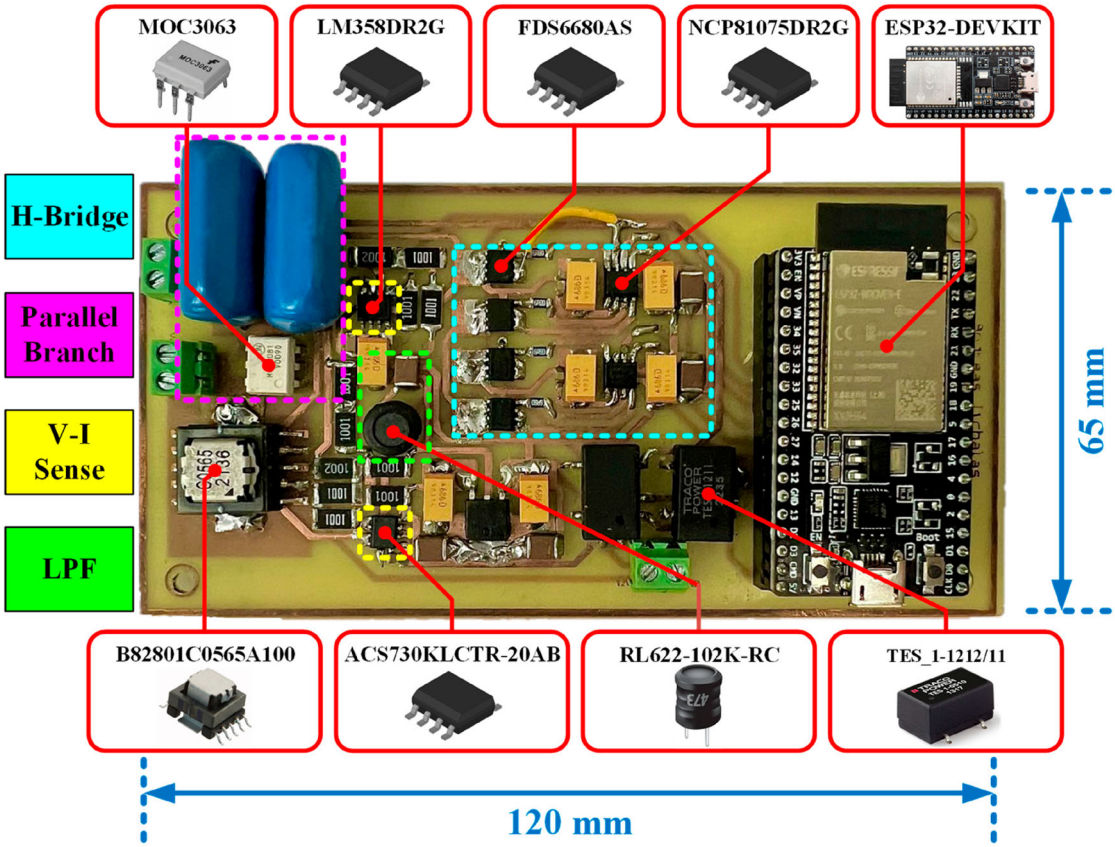

Figure 6. The developed hardware active fault detection kit.

Table 3. Main parameters of the experimental test bench.

Parameter / Description	Value [Unit]
Input supply voltage	12 [V]
Magnitude of injected voltage	2 [V]
Injection frequency	600 [Hz]
Grid voltage	24 [V_{rms}] (230 V / 24 V transformer)
Grid fundamental frequency	50 [Hz]
Installation load	Parallel combination: 50 [Ω] // 1 [mH]
Ground resistance	25 [Ω]
Injection period	0.4 [s]
Injection time interval	0.2 [s]
Ground impedance threshold NO_{Ulim}	20 [Ω]
Islanding impedance threshold ND_{Ulim}	50 [Ω]

above-described hardware prototype of the fault detection kit. Table 3 summarizes the main parameters of the experimental test bench.

The value of grounding resistance is of considerable importance in the event of unintentional neutral loss, as it leads to an additional voltage drop at its terminals, thereby reducing the line current. In Figure 7, both the output current of the H-bridge inverter (I_{inj}) and the line current (I_{Line}) that supplies the load are illustrated, for a neutral conductor loss scenario. Under normal operation of the utility grid, the coupling of the two harmonic components is evident, with the 50 Hz component manifesting as local peaks atop the 600 Hz component of the inverter signal. However, during a neutral loss event, there is a notable decrease in the amplitude of the 50 Hz component. Although this faulty condition can be easily detected by conventional protection devices (due to the single-phase configuration of the experimental test bed), it is examined here to validate the effective operation and interoperability of the proposed device. Additionally, it is worth mentioning that the modulation index (m_a) of the H-bridge inverter's SPWM has been carefully set at 0.2, ensuring that the amplitude of the fundamental harmonic component of the inverter remains low (below 2.5 V), to avoid affecting the operation of the current transformer.

Similar results are expected in the case of power theft through the simultaneous bridging of input-output phase and neutral terminals. Figure 8 presents both the output current of the H-bridge inverter (I_{inj}) and the line current (I_{Line}) that feeds the load, for the meter tampering case. During a power theft event, where conventional protection devices tent to fail to recognize this fault, the proposed kit is able to sense a current value higher than its predetermined threshold values, referred to power theft attempts.

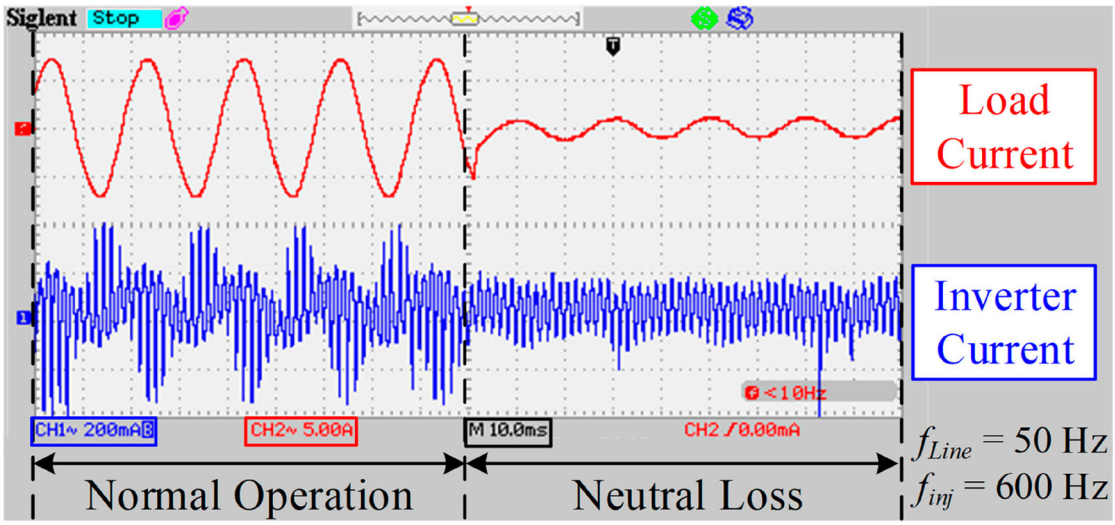

Figure 7. Experimental waveforms of the H-bridge inverter output and line currents, for the case of a neutral loss event.

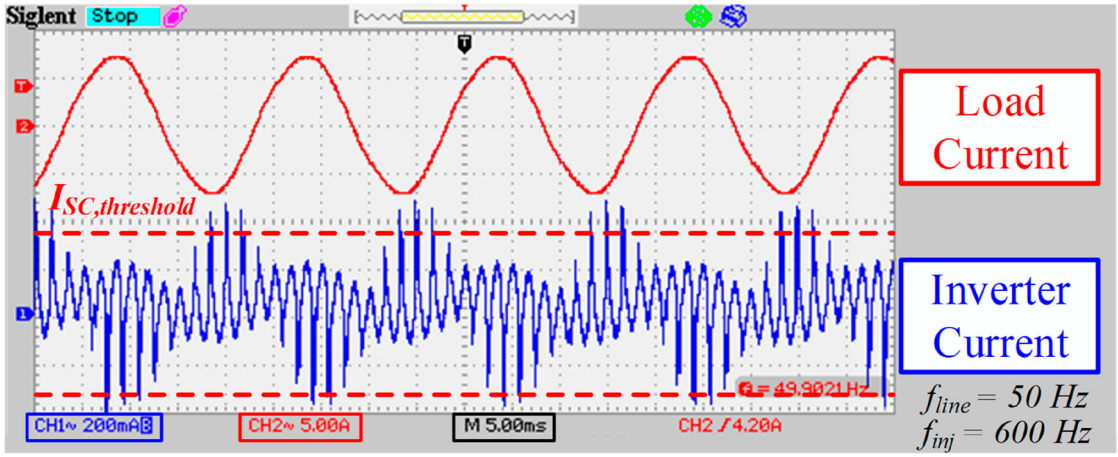

Figure 8. Experimental waveforms of the H-bridge inverter output and line current, for the case of a power theft event via the simultaneous bridging of the input-output phase and neutral terminals.

Subsequently, in Figure 9, the result of the Goertzel algorithm is depicted, facilitating the computation of the 50 Hz current amplitude, during an occurrence of neutral loss, as shown on the serial plotter of the Arduino IDE environment (ESP32 programming platform). Conversely, a notable decrease in the estimated line impedance is anticipated since these quantities exhibit an inverse relationship. The studied kit demonstrates its ability to accurately identify and quantify variations associated with a loss of neutral conductor. Therefore, an alert is issued to inform the user for this particular fault condition.

Under realistic conditions, the fault detection kit operates periodically, in predefined time slots, to minimize energy consumption. As it is depicted in Figure 10 (indicatively for the neutral conductor loss fault scenario), the device is programmed to operate for 0.5 s before entering an inactive state (deep sleep) for the subsequent 0.5 s, which confirms this intermittent mode of operation. The yellow and magenta waveforms depict the filtered output current and voltage from the inverter, respectively, whereas the light blue and green waveforms illustrate the line current and voltage, respectively. These signals alternate between periods of zero amplitude and times of normal injection. As stated in the ESP32 datasheet, the power consumption during deep sleep ranges from 10 μA to 150 μA, significantly less than the 160–260 mA consumption during continuous operation [55]. It is important to note that in realistic LV residential installations, such as ZEBs, these time intervals can be adjusted, to minimize the device power consumption since continuous operation is not necessary.

In conclusion, the IoT connectivity and communication capabilities of the smart kit are assessed through the uploading of the acquired measurements to the ThingSpeak web platform. The scenario of neutral conductor loss is examined, capturing the signal waveforms of line and inverter currents, as previously illustrated in Figures 7 and 10. Utilizing the Goertzel algorithm, the magnitude of the 50 Hz voltage and current components is determined. Following the necessary calculations, the microcontroller (connected to a Wi-Fi network) transmits the data to a ThingSpeak platform

Figure 9. The result of the Goertzel algorithm for the 50 Hz current component, displayed in the serial plotter of the Arduino IDE environment.

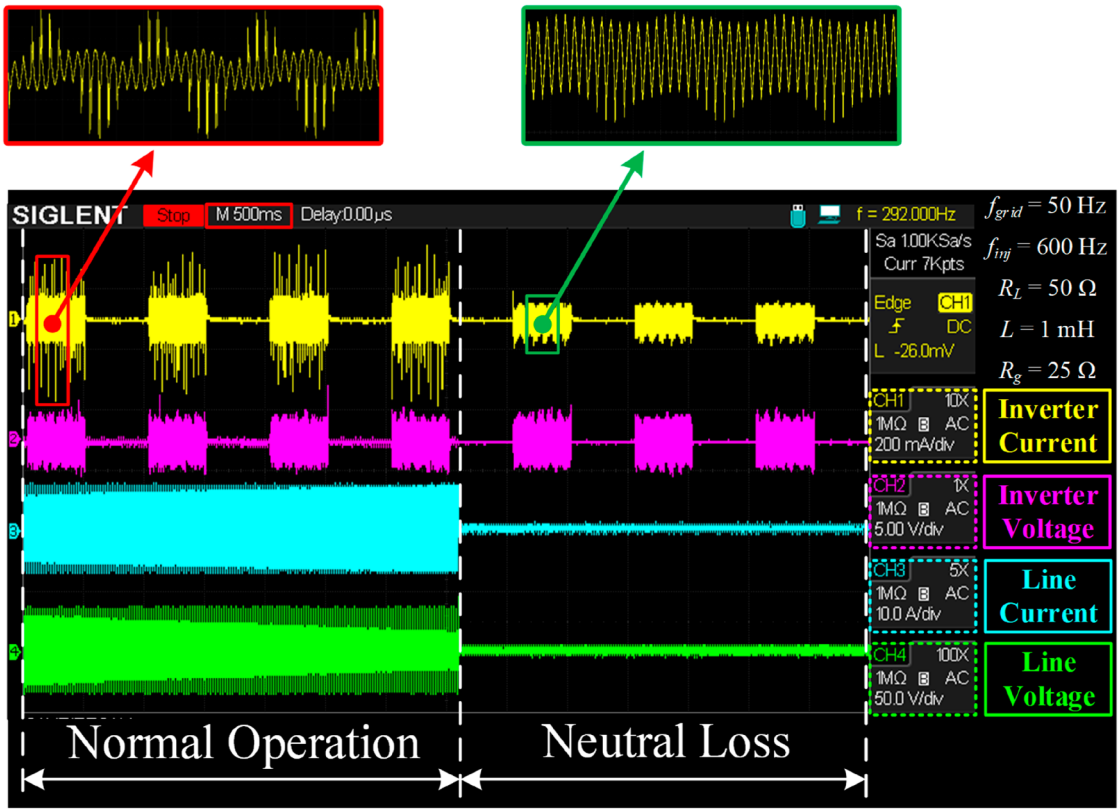

Figure 10. Experimental waveforms for the intermittent operation (deep sleep mode) of the kit, in case of the neutral conductor loss fault.

channel. The outcome of this process is illustrated in Figure 11, displaying the ThingSpeak webpage user interface. Two separate time charts demonstrate the line current at 50 Hz (Field Chart 1/blue waveform) and the estimated 600 Hz line impedance (Field Chart 2/red waveform) for the neutral loss scenario. It is evident, as previously mentioned, that the line current and line impedance feature an inverse relationship.

Thus, this straightforward IoT communication method empowers users to stay updated on their electrical installations' status (such as power consumption, current and voltage values, impedance value, and faults), at all times. In parallel, the existing smart meters can leverage this data to cross-validate their measurements, improving energy metering liability even further.

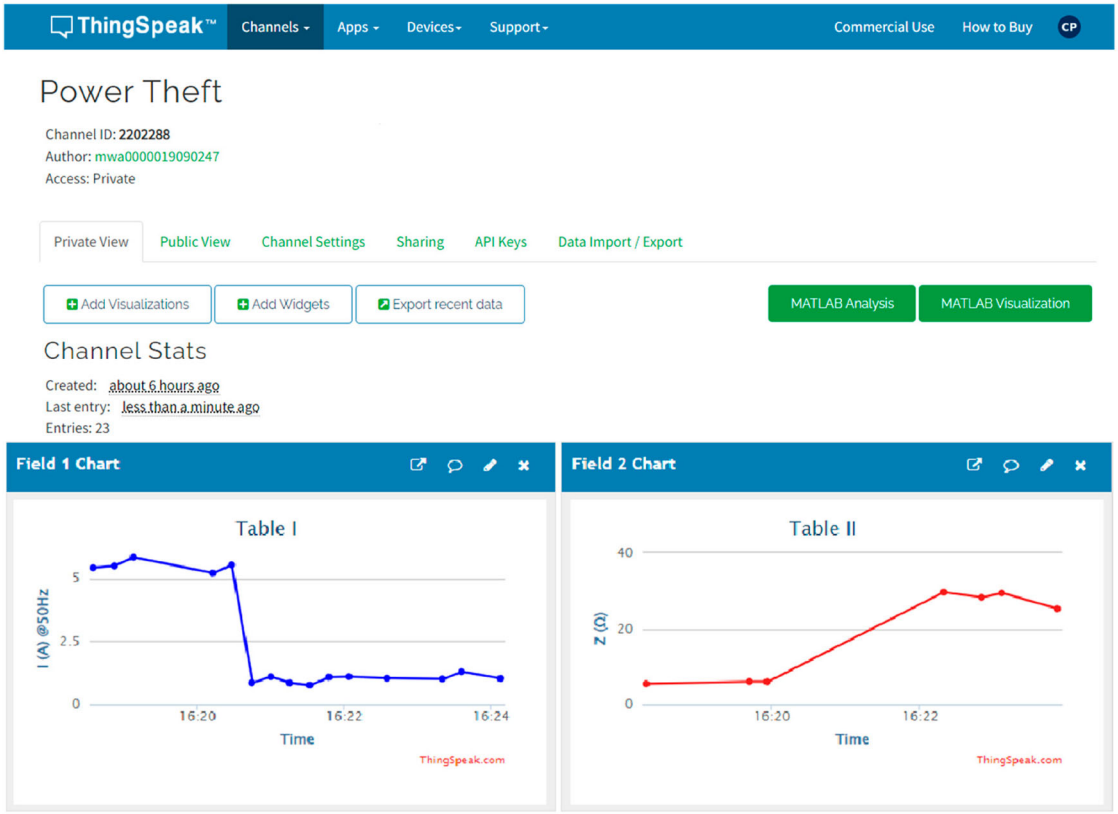

Figure 11. Line current (50 Hz) and estimated (600 Hz) grid impedance waveforms, as they are uploaded and displayed in ThingSpeak web platform.

4. Life cycle cost analysis

In this section, the LCCA of the active fault detection kit is presented. The aim of the analysis is to present the sustainability of the initial investment from the point of the investor, as well as the profit from the point of the manufacturing company. The LCCA analysis refers to the overall anticipated operating life of the first ten (10) years of installation and operation of the studied device.

The study will be conducted for the entire LV electrical distribution network in Greece, to capture the expected benefit from the kit in a real extent. It is noted that the investor is the Hellenic Electricity Distribution Network Operator (HEDNO S.A.). Thus, the proposed investment refers to a total number 4.7 million kits, that will be installed within a time period of 7 years (500,000 kit installations in the first year and 700,000 kits per year, for the rest six years). Considering the development and installation costs, the total initial cost of the active fault detection kit is roughly 242 €. Finally, the annual electrical energy consumption of each kit is 1.8 kWh, assuming that the installed kits operate intermittently by a duty cycle of 50%. A cost breakdown for the overall production and installation costs of the proposed kit is presented in Table 4. Except for the overall cost of 242 €, the maintenance / firmware upgrade (on average 0.5 man-hour of a technician) and replacement in case of damage (rate of 0.1% per year) costs are estimated at 8 and 0.25 € per year (according to the Manufacturer's internal calculations).

The present techno-economic analysis considers the aforementioned data, production, installation, maintenance and replacement costs in their net present value, as well as actual economic and time parameters presented in Table 5. The detailed equations of the LCCA methodology used in this work are presented in [56]. The outcome of the above analysis is the calculation of the total cost of the investment, during the whole life period.

As it was mentioned above, the present work assesses the sustainability of the investment, considering the economic cost / benefit from the point of the manufacturing company. Therefore, four scenarios of the initial kit cost increase are examined, such as 15%, 25%, 50% and 70%, in order to estimate the sustainability of the investment in case of alterations in the Electronics Market. Moreover, as for the operational costs of the proposed device, three scenarios (low, medium, high) of electricity price are considered, i.e. 0.105, 0.409 and 1.0 €/kWh. Finally, as Table 5 presents, five scenarios of rate of investment subsidy are examined. The case study is examined according to the official national (provided by the Regulatory Authority of Energy) electricity theft data of 2021, where the cost of non-technical electricity losses for this year was approximately at 209 million € [57]. Therefore, the net present value

Table 4. Cost breakdown for the development and installation costs of the active fault detection kit.

Cost category	Description	Cost (€)
Components	Semiconductors, passives, sensors, microcontroller, PCB etc.	40.7 *(as in* Table 2*)*
Packaging	Enclosure, terminals, harness, cabling etc.	20
Labor	Personnel cost for kit assembly and packaging.	50
Production Indirect	Testing, quality control, warehouse management, operational etc.	110.7 *(set at 100% of the direct production cost)*
Transport	Average price for kit transportation throughout the Greek territory.	5
Installation	Personnel cost for kit installation.	8
Installation Indirect	Value chain maintenance, warehouse management, operational etc.	7.8 *(fixed at 60% of the direct installation cost)*
Total		**≈ 242**

Table 5. Financial and time parameters of the LCCA.

Economic parameters	
Discount rate, *d*	0.25%
Inflation rate, *g*	4.6%
Escalation of energy costs	0.5%
Borrowing rate	0%
Rate of Investment subsidy, *i*	0%, 10%, 25%, 30% and 40%
Time parameters	
Period of analysis	10 years
Starting year	2024

of the annual benefit from reducing the electricity network non-technical losses is presented in Figures 12–14, leading to a cost of 2.224 billion € at the end of the 10 years period of the analysis. Finally, it is noted that based on the aforementioned data, the annual benefit corresponds to the reduction of non-technical losses by 90%. The results of the LCCA analysis are presented in Figures 12–14 for all the above-mentioned scenarios. These results are summarized in Table 6. Moreover, the total cost at the end of the life cycle of each scenario is provided. In accordance with the LCCA outcomes, all scenarios seem to be sustainable, considering that the payback period is achieved between 3 and 4 years, even in the worst case of 0% rate of subsidy.

5. Conclusion

An active fault detection kit oriented to modern ZEB installations is studied, capable of detecting meter tampering, neutral conductor loss and unintentional islanding. This device periodically injects a harmonic voltage component at the phases of an electrical installation and by monitoring the circuit impedance and current, it diagnoses and classifies the fault type; the power flow of the installation at the fundamental frequency remains unaffected from the harmonic voltage injection, by utilizing a single current transformer. Moreover, a solution about the impedance estimation under zero / low load conditions is presented, by introducing a parallel branch, comprising a capacitor, in series with a TRIAC switch.

In contrast to prevalent methodologies, dominantly relying on the harmonic current injection, the proposed kit utilizes a series harmonic voltage injection mechanism, offering a comprehensive solution regarding the issues of unintentional islanding and neutral conductor loss, in the context of current and future ZEB electrical installations and the prospect of mass installation of DGs and storage units. In parallel, the proposed device is able to detect directly and reliably

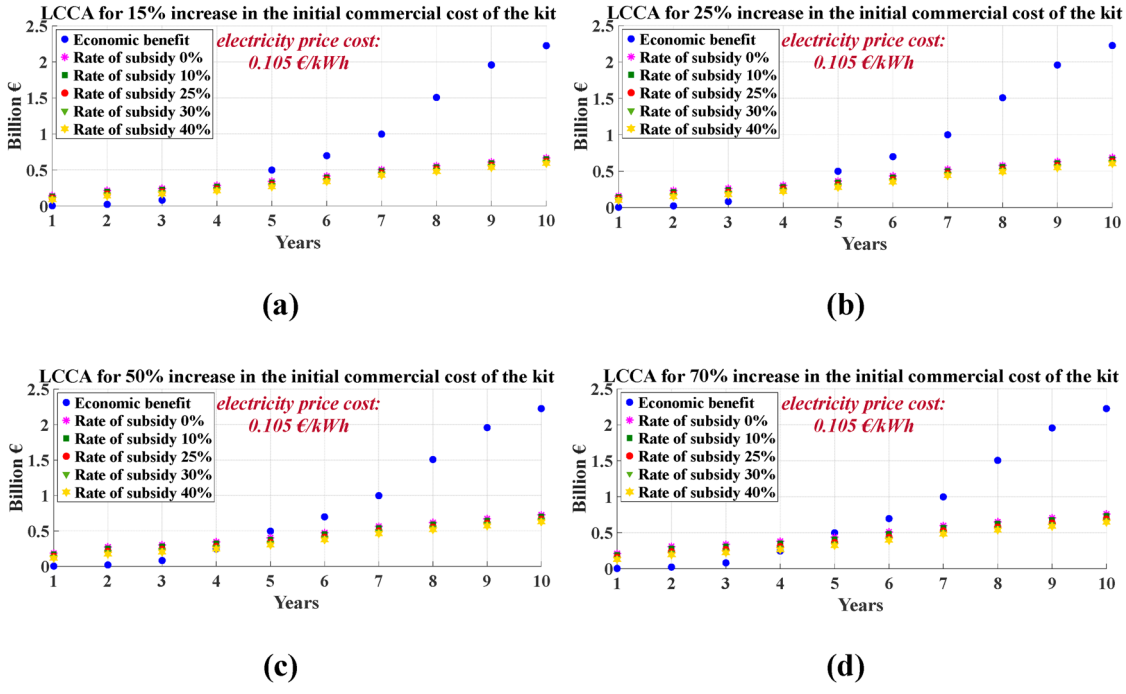

Figure 12. LCCA results for electricity price cost scenario 0.105 €/kWh.

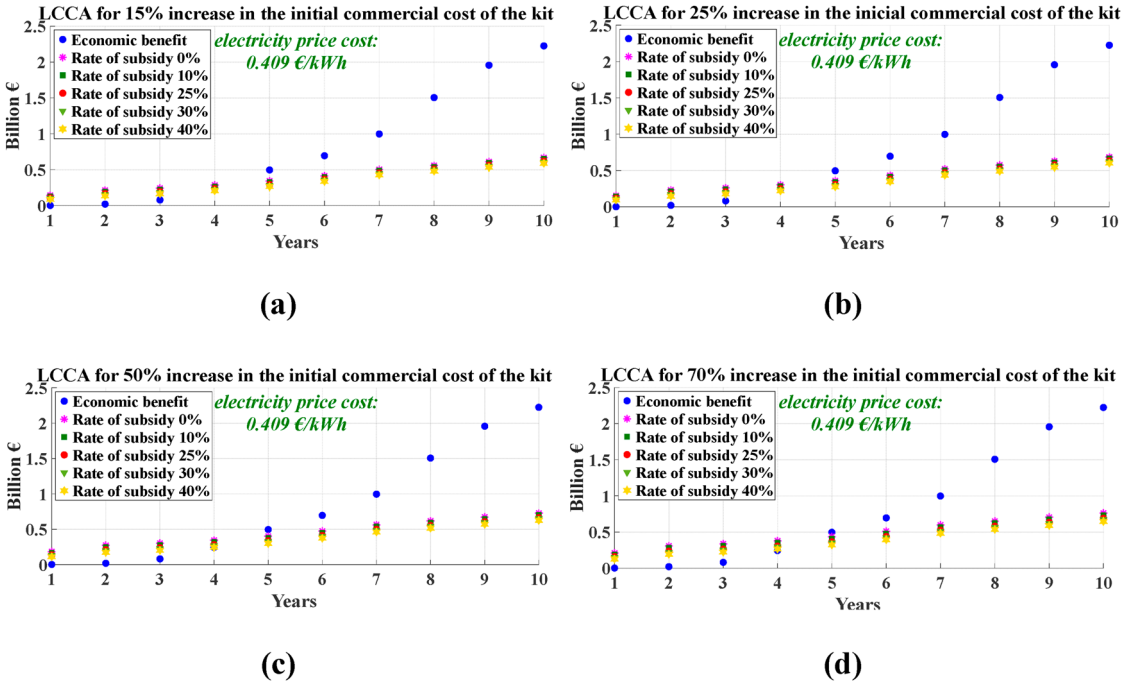

Figure 13. LCCA results for the electricity price cost scenario of 0.409 €/kWh.

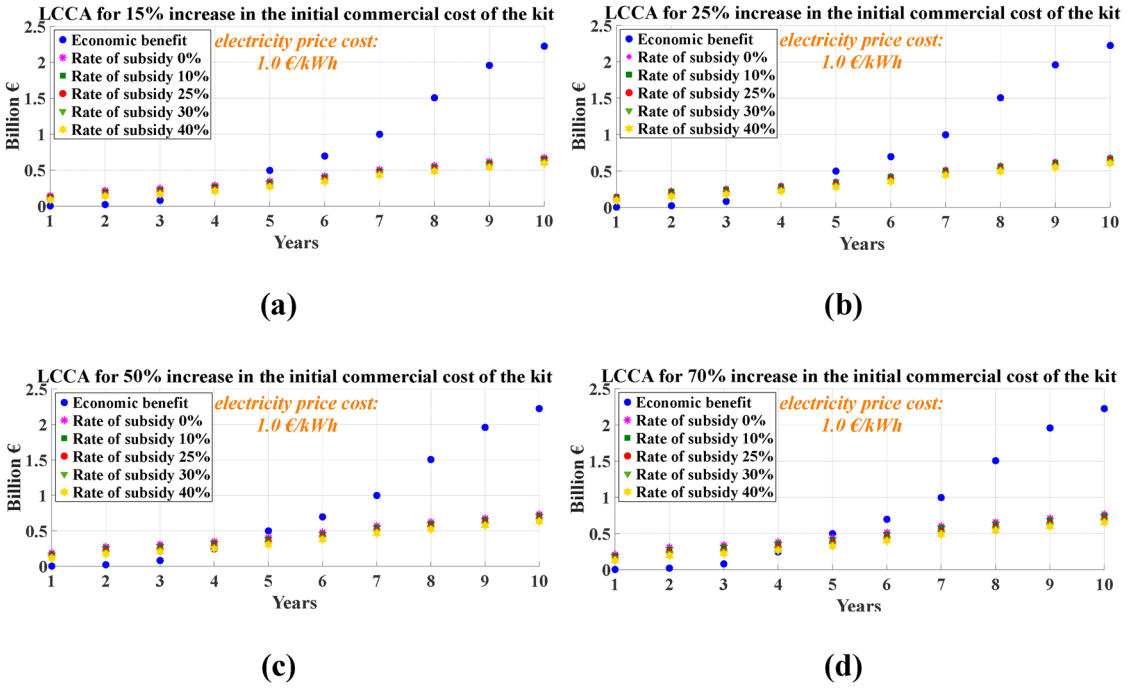

Figure 14. LCCA results for the electricity price cost scenario of 1 €/kWh.

any meter tampering attempt without involving complex algebra or computationally intensive data analysis methods, by the aid of the powerful, robust and fast Goertzel algorithm. Compared to previous works, the adoption of this algorithm facilitates the straightforward and efficient digital implementation, leading to minimum computational burden.

For example, statistical methods could be used to analyze the distribution of smart meter recordings, to detect outliers or unexpected changes, whereas numerical methods could be used too, utilizing algorithms to solve equations that model the normal operation of the meter and identify deviations. Although, both methods encounter limitations, since they involve approximations and assumptions, which introduce uncertainties. In addition, they can be computationally intensive, introducing complexity and require significant expertise to implement correctly. Finally, it is worth noting that their effectiveness depends on the quality and quantity of the available data. Hence, by accommodating the fast, simple and robust Goertzel algorithm and by not relying on the above-mentioned methods,

Table 6. LCCA results. Total cost the end of the life cycle and payback period, for each scenario.

		Electricity Price [€/kWh]					
		0.105		0.409		1	
Rate of Subsidy [%]	Profit Increase [%]	Total Cost [M€]	Payback [Years]	Total Cost [M€]	Payback [Years]	Total Cost [M€]	Payback [Years]
0	**15**	667.67	4	669.33	4	672.57	4
	25	684.62	4	686.29	4	689.52	4
	50	727.01	4	728.67	4	731.91	4
	70	760.92	4	762.58	4	765.82	4
10	**15**	648.22	4	649.89	4	653.12	4
	25	663.48	4	665.15	4	668.38	4
	50	701.64	4	703.31	4	706.54	4
	70	732.17	4	733.83	4	737.07	4
25	**15**	619.05	3	620.71	3	623.95	3
	25	631.78	4	633.44	4	636.68	4
	50	663.59	4	665.25	4	668.49	4
	70	689.04	4	690.71	4	693.94	4
30	**15**	609.32	3	610.99	3	614.22	3
	25	621.21	3	622.87	3	626.11	3
	50	650.91	4	652.57	4	655.81	4
	70	674.67	4	676.33	4	679.57	4
40	**15**	589.88	3	591.54	3	594.78	3
	25	600.07	3	601.73	3	604.97	3
	50	625.54	3	627.20	3	630.44	3
	70	645.92	4	647.58	4	650.82	4

the proposed kit aims to provide a more direct and potentially more reliable means of detecting faults, through data monitoring via direct measurement techniques. Last, but not least, it is noted that the selected Goertzel algorithm (which is basically a form of the discrete Fourier transformation that extracts the phase and magnitude of an input signal, at a desired frequency) constitutes a special and powerful method for computing the signal spectra, using a digital filtering method, without involving complex algebra, like the DFT algorithm.

The efficacy of the proposed kit is studied and validated in a single-phase experimental setup. Apparently, the proposed kit can be seamlessly integrated in the circuit of a smart meter, or operate in coordination with any existing energy meter in the installation, providing fault warnings. The latter feature is facilitated by the advanced features of the selected ESP32 microcontroller, such as its IoT communication capabilities, which are experimentally tested and highlighted. Finally, the sustainability of the developed prototype is assessed by means of an insightful LCCA. In essence, the studied fault detection kit is proved to be a compact and flexible device, boasting extensive connectivity options and offering a holistic solution for the issues of islanding, neutral loss, and power theft, in the prospect of future ZEB installations.

Disclosure statement

No potential conflict of interest was reported by the author(s).

Funding

This research has been co-financed by the European Regional Development Fund of the European Union and Greek national funds through the Operational Program East Macedonia and Thrace 2014–2020, under the call "Investment Plans for Innovation, Research and Development of Companies in the Branch of Electronics and Electrical Equipment Production" (project code: AMTH3-0063343).

ORCID

Nick Rigogiannis http://orcid.org/0000-0002-3056-5606
Nick Papanikolaou http://orcid.org/0000-0001-8546-1196

References

[1] Minelli F, Ciriello I, Minichiello F, et al. From net zero energy buildings to an energy sharing model - The role of NZEBs in renewable energy communities. Ren Energy. 2024;223:120110. doi:10.1016/j.renene.2024.120110
[2] Hu K, Yan C, Xu C, et al. Strategies for grid-friendly and uncertainty-adaptive design in zero energy buildings. Energy Build. 2024;307:113967. doi:10.1016/j.enbuild.2024.113967
[3] Rigogiannis N, Kotarela F, Boubaris A, et al. Incorporation of SmartPV Technology in zero energy building concept. 2022 22nd International Symposium on Electrical Apparatus and Technologies (SIELA), Bourgas, Bulgaria, 2022, pp. 1–4. doi:10.1109/SIELA54794.2022.9845757
[4] Frantzeskakis S, Voglitsis D, Papanikolaou N, et al. Loss of neutral in low voltage electrical installations with connected DG units - consequences and solutions. 25th Int. Conf. Electricity Distrib. 2019:1–5.
[5] Cohen V. Loss of neutral in low voltage distribution systems - consequences and solutions. CBI Electric Report, pp. 1–8.
[6] Lepadat I, Helerea E, Abagiu S. Effect of the neutral interruption on the unbalanced three-phase consumers. 2014 International Conference on Optimization of Electrical and Electronic Equipment, Bran, Romania, 2014, pp. 192-197.
[7] Amhenrior HE, Edeko FO, Ogujor EA, et al. Design and implementation of an automatic tamper detection

and reporting capability for a single phase energy meter. 2017 IEEE 3rd International Conference on Electro-Technology for National Development, Owerri, Nigeria, 2017, pp. 1–9.
[8] Shahzad Gill T, Shehwar DE, Memon H, et al. IoT based smart power quality monitoring and electricity theft detection system. 2021 16th International Conference on Emerging Technologies, Islamabad, Pakistan, 2021, pp. 1–4.
[9] Kulkarni AU, Jayalaxmi GN. IoT Solution for Live Wire Tampering. 2018 IEEE Punecon, Pune, India, 2018, pp. 1–7.
[10] Voglitsis D, Valsamas F, Rigogiannis N, et al. On harmonic injection anti-islanding techniques under the operation of multiple DER-Inverters. IEEE Trans Energy Conv March 2019;34(1):455–467. doi:10.1109/TEC.2018.2881737
[11] Guo Z. A harmonic current injection control scheme for active islanding detection of grid-connected inverters. 2015 IEEE International Telecommunications Energy Conference, Osaka, Japan, 2015, pp. 1–5.
[12] Valsamas F, Voglitsis D, Rigogiannis N, et al. Comparative study of active anti-islanding schemes compatible with MICs in the prospect of high penetration levels and weak grid conditions. IET Gener Transm Distrib. 2018;12:4589–4596. doi:10.1049/iet-gtd.2018.5636
[13] Kunte RS, Gao W. Comparison and review of islanding detection techniques for distributed energy resources. 2008 40th North American Power Symposium, Calgary, AB, Canada, 2008, pp. 1–8.
[14] Messinis G, Hatziargyriou N. Review of non-technical loss detection methods. Electric Power Syst Res May 2018;158:250–266. doi:10.1016/j.epsr.2018.01.005
[15] Rigogiannis N, Pechlivanis C, Tichalas A, et al. On the design of an Islanding, neutral loss and meter tampering detection kit for low voltage electrical installations. 2023 International Conference on Electrical Drives and Power Electronics (EDPE), The High Tatras, Slovakia, 2023, pp. 1–7.
[16] Frantzeskakis S, Rigogiannis N, Christodoulou C, et al. On the detection of neutral loss, islanding, and meter tampering in electrical installations. IEEE Open J Ind Electron Soc. 2024;5:1–12. doi:10.1109/OJIES.2024.3354799
[17] Directive 2018/844/EU 2010 European Parliament and of the Council of 30 May 2018 amending Directive 2010/31/EU.
[18] Deshbhratar P, Somalwar R, Kadwane SG. Comparative analysis of islanding detection methods for multiple DG based system. 2016 International Conference on Electrical, Electronics, and Optimization Techniques, Chennai, India, 2016, pp. 1525–1530.
[19] Kodakkatery M, Bavisetti K. Emerging Market Smart Grid: Outlook 2015. study by Northeast Group LLC. 2015.
[20] Zhang QY, Dai J, Liu B, et al. A power theft detection algorithm based on electricity usages, 2022 2nd International Conference on Algorithms, High Performance Computing and Artificial Intelligence (AHPCAI), Guangzhou, People's Republic of China, 2022, pp. 115–120. doi:10.1109/AHPCAI57455.2022.10087801
[21] Shahid MB, Shahid MO, Tariq H, et al. Design and development of an efficient power theft detection and prevention system through consumer load profiling. 2019 International Conference on Electrical, Communication, and Computer Engineering (ICECCE), Swat, Pakistan, 2019, pp. 1–6. doi:10.1109/ICECCE47252.2019.8940644
[22] Gupta AK, Mukherjee A, Routray A, et al. A novel power theft detection algorithm for low voltage distribution network. IECON 2017 - 43rd Annual Conference of the IEEE Industrial Electronics Society, Beijing, China, 2017, pp. 3603–3608. doi:10.1109/IECON.2017.8216611
[23] Pavithra KN, Tarunkumar S, Nesakumar D, et al. GPS-based power theft detection and alert system using GSM. 2023 International Conference on Research Methodologies in Knowledge Management, Artificial Intelligence and Telecommunication Engineering (RMKMATE), Chennai, India, 2023, pp. 1–3. doi:10.1109/RMKMATE59243.2023.10368907
[24] Luan W, Wang G, Yu Y, et al. Energy theft detection via integrated distribution state estimation based on AMI and SCADA measurements. 2015 5th International Conference on Electric Utility Deregulation and Restructuring and Power Technologies (DRPT), Changsha, China, 2015, pp. 751–756. doi:10.1109/DRPT.2015.7432350
[25] McLaughlin S, Holbert B, Fawaz A, et al. A multi-sensor energy theft detection framework for advanced metering infrastructures. IEEE J Sel Areas Commun. July 2013;31(7):1319–1330. doi:10.1109/JSAC.2013.130714
[26] Zheng K, Chen Q, Wang Y, et al. A novel combined data-driven approach for electricity theft detection. IEEE Trans Ind Inf. March 2019;15(3):1809–1819. doi:10.1109/TII.2018.2873814
[27] Yan Z, Wen H. Performance analysis of electricity theft detection for the smart grid: an overview. IEEE Trans Instrum Meas. 2022;71:1–28. Art no. 2502928, doi:10.1109/TIM.2021.3127649
[28] Christopher AV, Swaminathan G, Subramanian M, et al. Distribution line monitoring system for the detection of power theft using power line communication. 2014 IEEE Conference on Energy Conversion (CENCON), Johor Bahru, Malaysia, 2014, pp. 55–60. doi:10.1109/CENCON.2014.6967476
[29] Chen Y, Hua G, Feng D, et al. Electricity theft detection model for smart meter based on residual neural network. 2020 12th IEEE PES Asia-Pacific Power and Energy Engineering Conference (APPEEC), Nanjing, China, 2020, pp. 1–5. doi:10.1109/APPEEC48164.2020.9220523
[30] Gui R, Zhang X, Gui X. A federal learning framework for privacy-protected distributed power theft detection. 2024 IEEE 14th International Conference on Electronics Information and Emergency Communication (ICEIEC), Beijing, China, 2024, pp. 1–4. doi:10.1109/ICEIEC61773.2024.10561759
[31] Huang L, Qin H, Pan Z, et al. Electricity theft detection based on iterative interpolation and fusion convolutional neural network. 2022 7th International Conference on Power and Renewable Energy (ICPRE), Shanghai, China, 2022, pp. 567–571. doi:10.1109/ICPRE55555.2022.9960403
[32] Lingqing G, Xiaobin C, Zhaoming L, et al. Detection method for power theft based on SOM neural network and K-means Clustering Algorithm. 2019 22nd International Conference on Electrical Machines and Systems (ICEMS), Harbin, China, 2019, pp. 1–5. doi:10.1109/ICEMS.2019.8922302
[33] Wang Z, Kong X, Yang Z, et al. Electricity theft detection and classification method based on D-S Feature Fusion and IALO-SVM. 2022 25th International Conference

on Electrical Machines and Systems (ICEMS), Chiang Mai, Thailand, 2022, pp. 1–5. doi:10.1109/ICEMS56177.2022.9983310

[34] Peng Y, Yang Y, Xu Y, et al. Electricity theft detection in AMI based on clustering and local outlier factor. IEEE Access. 2021;9:107250–107259. doi:10.1109/ACCESS.2021.3100980

[35] Abraham OA, Ochiai H, Hossain MD, et al. Electricity theft detection for smart homes: harnessing the power of machine learning with real and synthetic attacks. IEEE Access. 2024;12:26023–26045. doi:10.1109/ACCESS.2024.3366493

[36] Lin G, Feng X, Guo W, et al. Electricity theft detection based on stacked autoencoder and the undersampling and resampling based random forest algorithm. IEEE Access. 2021;9:124044–124058. doi:10.1109/ACCESS.2021.3110510

[37] Liao W, Yang Z, Liu K, et al. Electricity theft detection using Euclidean and graph convolutional neural networks. IEEE Trans Power Syst. July 2023;38(4):3514–3527. doi:10.1109/TPWRS.2022.3196403

[38] Abbas S, Bouazzi I, Ojo S, et al. Improving smart grids security: An active learning approach for smart grid-based energy theft detection. IEEE Access. 2024;12:1706–1717. doi:10.1109/ACCESS.2023.3346327

[39] Shahzad Gill T, Shehwar DE, Memon H, et al. IoT based smart power quality monitoring and electricity theft detection system. 2021 16th International Conference on Emerging Technologies (ICET), Islamabad, Pakistan, 2021, pp. 1–4. doi:10.1109/ICET54505.2021.9689908

[40] Ogu RE, Chukwudebe GA. Development of a cost-effective electricity theft detection and prevention system based on IoT technology. 2017 IEEE 3rd International Conference on Electro-Technology for National Development (NIGERCON), Owerri, Nigeria, 2017, pp. 756–760. doi:10.1109/NIGERCON.2017.8281943

[41] Press Release. Siemens launches Gridscale X™, paving the way for autonomous grid management. Siemens, Available from: https://press.siemens.com/global/en/pressrelease/siemens-launches-gridscale-xtm-paving-way-autonomous-grid-management.

[42] Press Release. SMART ENERGY SERVICES FOR UTILITY FIELD OPERATIONS. 2022, Available from: https://pmt.honeywell.com/content/dam/pmt/en/documents/gated/smart-energy-utility-services.pdf.

[43] Press Release. Accurately Identify, Manage and Prevent Energy Theft to Protect and Recover Revenues. LandisGyr+, 2015, Available from: https://www.landisgyr.ch/webfoo/wp-content/uploads/2015/01/PS_RevenueProtection.pdf.

[44] Brochure. Energy Meter Kits. Schneider Electric, 2019, Available from: https://download.schneider-electric.com/files?p_Doc_Ref=3000BR1801&p_enDocType=Brochure&p_File_Name_Energy+Meter+Kit+Brochure+%5Bdigital+file%5D.pdf.

[45] Press Release. Bidgely selected as the technology service provider for energy theft solution by ministry of power, gol in 'Powerthon 2022'. Bidgely, 2022, Available from: https://www.bidgely.com/bidgely-selected-for-energy-theft-solution-by-ministry-of-power/.

[46] Mesganaw M. How to detect and harden an electricity meter against tampering by neutral disconnection, application Note, Texas Instruments, 2020, Available from: https://www.ti.com/lit/wp/slyy184/slyy184.pdf?ts=1719964161324.

[47] Reference Design. Case tamper detection reference design using inductive sensing. Texas Instruments, 2017, Available from: https://www.ti.com/lit/ug/tidud41/tidud41.pdf?ts=1720024122469&ref_url=https%253A%252F%252Fwww.ti.com%252Ftool%252FTIDA-01377.

[48] Reference Design. Three-phase metrology with enhanced ESD protection and tamper detection. Texas Instruments, 2015, Available from: https://www.ti.com/lit/ug/tidu817/tidu817.pdf?ts=1720061497814&ref_url=https%253A%252F%252Fwww.ti.com%252Ftool%252FTIDM-3PHMTR-TAMP-ESD.

[49] Kim J-H, Kim J-G, Ji Y-H, et al. An islanding detection method for a grid-connected system based on the Goertzel algorithm. IEEE Trans Power Electron April 2011;26(4):1049–1055. doi:10.1109/TPEL.2011.2107751

[50] Asiminoaei L, Teodorescu R, Blaabjerg F, et al. A digital controlled PV-inverter with grid impedance estimation for ENS detection. IEEE Trans Power Electron Nov. 2005;20(6):1480–1490. doi:10.1109/TPEL.2005.857506

[51] Gonzalez SA, Garcia-Retegui R, Benedetti M. Harmonic computation technique suitable for active power filters. IEEE Trans Ind Electron Oct. 2007;54(5):2791–2796. doi:10.1109/TIE.2007.894789

[52] Standard E. Voltage characteristics of electricity supplied by public electricity networks, European committee for electrotechnical standardization (CENELEC). Standard EN. 2010;50160:2010.

[53] Kim J-H, Kim J-K, Jung Y-C, et al. A novel islanding detection method using Goertzel algorithm in grid-connected system. The 2010 International Power Electronics Conference, Sapporo, Japan, 2010, pp. 1994–1999.

[54] Rigogiannis N, Voglitsis D, Papanikolaou N. Microcontroller Based Implementation of Peak Current Control Method in a Bidirectional Buck-Boost DC-DC Converter. 2018 20th International Symposium on Electrical Apparatus and Technologies (SIELA), Bourgas, Bulgaria, 2018, pp. 1–4.

[55] Espressif Systems. ESP32 Series Datasheet; 2023. [Online]. Available: https://www.espressif.com/sites/default/files/documentation/esp32_datasheet_en.pdf.

[56] Kotarela F, Rigogiannis N, Glavinou E, et al. Techno-economic and environmental assessment of a photovoltaic-based fast-charging station for public utility vehicles. Energies. 2024;17(3):632. doi:10.3390/en17030632

[57] HEDNO S.A. Electricity theft. Available from: https://deddie.gr/en/kentro-enhmerwsis/reumatoklopes/.